International Journal of Advances in Engineering and Management (IJAEM)
Volume 7, Issue 07 July 2025, pp: 331-348 www.ijaem.net ISSN: 2395-5252

Integrated Geophysical Survey of Lower Benue Trough, Nigeria, Using Airborne Radiometric and Gravity Data

Diala, Chibueze Kenneth, Obiora, Nnaemeka Daniel, Ugbor, Okechukwu Desmond, Okwesili, NgoziAgatha and Ugwu, NgoziMirianrita

Department of Physics and Astronomy, University of Nigeria, Nsukka

---

Date of Submission: 01-07-2025 Date of Acceptance: 10-07-2025

ABSTRACT: The airborne radiometric and gravity data sheets of Agana, Gboko, Oturkpo, and Makurdiareas were interpreted to address the following objectives: estimating the depth to the basement (sedimentary thickness), determining the density contrast and the type of mineralization prevalent in the area, determining the radiometric mineralization content of potassium, uranium, and thorium (K, U, and Th) and delineating areas of radiometric anomalies. The data were grided and minimum curvature was applied to produce radiometric maps of potassium, uranium, thorium, radiometric ratio maps, and ternary maps. The three radioelements vary in concentrations systematically with one another, thus maintaining average constant ratios among them in all rock types. The analysis of radiometric data revealed that the thorium abundance compared with the standard radiometric table are related to the presence of sedimentary rocks such as limestone and clay mostly in the Makurdi area, and sandstone in the Gboko area. In contrast, the Oturkpo area with high concentrations of Thorium abundance (above 17.5 ppm) is possibly sedimentary rocks. The low concentration of K abundance is dominant in the northern part of the Agana area with the presence of igneous rocks while the high concentration of K abundance is dominant in the Makurdi area which are likely sedimentary rocks. The source parameter imaging depthranges from -392.7 to -5159.5 m indicating the depth of potential field sources or estimated depth to the basement (sedimentary thickness) while the Euler deconvolution ranges from 929.1 to -4442.1 m indicating the nature and corresponding depths of the geologic sources. The forward and inverse modeling employed the trial-and-error method for the modeled profiles P1, P2, P3, and P4, with respective depths of -1706, -3702, -2451, and -1146m. The density values were 2.51, 2.19, 2.62 and 2.53g/cm^3. The result from the forward and inverse modeling analysis indicated the presence of rock-bearing minerals like granite, limestone, shale, clay, and sandstone.Therefore, the research area has identified rock-bearing mineral deposits that could be utilized as raw material(s) by numerous companies and industries in Nigeria. The maximum sedimentary thickness of 4907.9m obtained indicates the possibility of hydrocarbon accumulation and exploration in the area.

Keyword: Radiometric Maps, Radiometric Ratio Maps, Ternary Map, Gravity Anomaly, Euler Deconvolution, Source Parameter Imaging, Forward and Inverse Modeling.

I. INTRODUCTION

Airborne geophysical survey is a process of measuring the variation of the earth's surface from an aeroplane. It is commonly used in mineral exploration projects to measure the physical properties of the ground to provide information on the geology. The surveys can measure the natural earth's fields such as magnetic, gravity and radiometric. Murphy (2007) stated that airborne geophysical surveys help in the search for petroleum resources and other mineral deposits and in general, airborne surveys are used at the early stages of exploration to cover or study extensive areas or large areas (reconnaissance survey). Generally, the application of airborne surveys has no environmental effect on the acquisition of data. To achieve this, data are obtained from the earth's surface using airborne and when analyzed, are used to study or reveal the internal structures of the earth (rocks and minerals). In the same vein, geophysics seeks to look for contrast in rock properties associated with uncommon specific structures, which can contain the minerals being sought (Telford et al., 1990; Lowrie, 2007). The interpretation of the measured and recorded data in terms of variations in their physical properties reveals the anomalies, hence, minerals present in that area.

Radiometric survey studies the geologic lithology and different rock types formed from the distinctive radioelements content signature. There are more than fifty naturally occurring radioactive isotopes, but the majority are rare or only very weakly radioactive. The elements of principal interest in radiometric exploration are potassium ^{40}K, uranium ^{235}U, and thorium ^{232}Th. The three radioelements (^{40}K, ^{235}U and ^{232}Th) in rocks vary in concentrations systematically with one another thus maintaining average constant ratios among them in all rock types. The radiometric method is a technique used to determine radiometric anomalies and the observed minerals. The naturally occurring elements are known to be radioactive and every detectable gamma radiation from the earth's materials comes from the natural decay products of only these three elements; potassium, uranium, and thorium (Telford et al., 1990). Perhaps, many naturally occurring elements have radioactive isotopes, but only these three elements (potassium, uranium, and thorium) Decay series have radioisotopes that produce gamma rays of sufficient energy and intensity, which are measured in gamma-ray spectrometer during the survey. The acquisition of radiometric data is usually collected above the ground by drone or helicopter installed with spectrometers on it and continuous operations of the gamma-ray spectrometers along equally spaced parallel flight lines covering the survey location, which is the same as the radiometric survey carried out with a hand-held spectrometer, allows many vast areas of the earth's surface to be quickly acquired. The aircraft lines in a grid-like pattern with height and line spacing, which determine the resolution of the data.

Gravity surveying measures the gravitational attractions of rocks by measuring the variation in the pulls of gravity within the earth's surface. Gravity survey is a geophysical method applied in modern geologic mapping and hydrocarbon recovery with its operating principle similar to that of the ground gravity survey, but explores very large uninvestigated and inaccessible locations of interest within a short period, thereby making the method cheaper and faster. Gravity survey investigates the internal structure of the earth's surface based on the gravitational field variations that occur due to the gravity properties of rocks that sequestrate the earth's surface caused by lateral density contrast. It can be interpreted to delineate the minerals and rocks that triggered the anomalies in the variation of the earth's gravitational field. The gravity data is collected by installing the gravimeter in a drone or helicopter and continuous operations of this gravimeter along equally spaced parallel flight lines covering the survey locations, which is similar to a gravity survey carried out with a handheld gravimeter, allows many vast locations of the earth's surface to be covered. The aircraft flies in a grid-like pattern with height and line spacing determining the resolution of the data and as the aircraft flies, the gravimeter records tiny variations in the density contrast of the ambient gravitational field due to the temporal effects of the frequently varying gravitational field.

For this reason, gravity instruments are designed to measure the variation in the force of gravity from one place to another rather than the absolute force of gravity itself. The gravity method has been used extensively in the search for oil and gas in the twentieth century and the seismic method is the current method employed in the search for oil and gas and, enhanced oil recovery (Telford et al., 1990).

This paper aims at interpreting qualitatively and quantitatively the airborne radiometric and gravity data of the Agana, Oturkpo, Gboko, and Makurdi areas in the Lower Benue Trough, Nigeria. The specific objectives include to: (i) estimate the depth to the basement (sedimentary thickness), (ii) determine the density contrast and type of mineralization prevalent, (iii) determine the radiometric mineralization content of K-potassium, U-uranium, and Th-thorium and (iv) delineate the areas of radiometric anomalies in the study area.

LOCATION AND GEOLOGY OF THE LOWER BENUE TROUGH

The Lower Benue Trough has geological structures underlying a large part of Nigeria and extending about 1,000 km northeast. The trough has its southern limit at the northern boundary of the Niger Delta and it is divided into lower, middle, and upper regions. The study area as shown in the geology map (Fig 1.1) is bounded by latitude 7.0° and 8.0° N and longitude 8.0° E and 9.0° E. The erosion of the Abakaliki uplifted and folded belts resulted in the development of a Proto-Niger Delta sequence consisting of Enugu/Agwu and Ezeaku

International Journal of Advances in Engineering and Management (IJAEM)
Volume 7, Issue 07 July 2025, pp: 331-348 www.ijaem.net ISSN: 2395-5252

formations. The Lower Benue Trough like other Sedimentary Basins in Nigeria is found to be endowed with mineral resources. Over twenty mineral resources have so far been reported in the Trough by the Nigeria Geological Survey Agency NGSA and these include; coal, lead, zinc, barytes, limestone, clay, gypsum, phosphate, glass sand, fluorspar, salt, ironstone, uranium, sulphur, graphite, cassiterite, manganese, mica and silver (Fatoye& Gideon, 2013). The Lower Benue Trough is a geological feature located in Nigeria, West Africa. It is part of the larger Benue Trough, which extends across several countries, including Nigeria, Cameroon, Chad, and Niger. The trough also has significant hydrocarbon potential and there have been explorations for oil and gas within the basin, and some successful oil discoveries have been made in the region (Fatoye& Gideon, 2013). The basin has gigantic economic benefits and has increased foreign exchange revenues in the entire Lower Benue Trough.

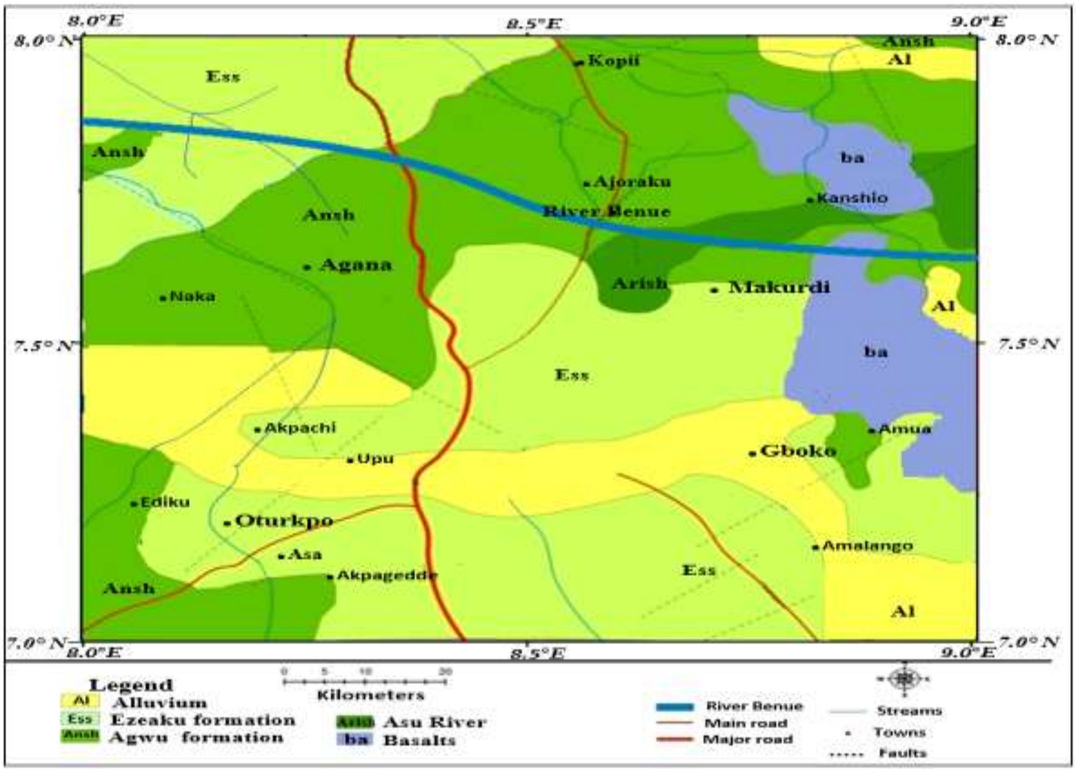

Figure 1: Geologic map of the study area.

II. MATERIALS AND METHODOLOGY

MATERIALS

Four sheets were used and include Agana (sheet 250), Makurdi (sheet 251), Oturkpo (sheet 270) and Gboko (sheet 271). The radiometric and gravity data were all digitized and presented in XYZ Geosoft format, where X is the latitude, Y is the longitude and Z is the field intensity. The method involves interpreting geophysical survey using Oasis Montaj software (8.4 version) for the identification of rocks variation in concentrations and to delineate the minerals and rocks that triggered the anomalies in the variation of the earth's gravitational field.

METHODS OF RADIOMETRIC DATA INTERPRETATION

Radiometric Ratio Maps

Uranium (U), Thorium (Th) and Potassium (K) are the three most common naturally occurring radionuclides on the surface of Earth. They are used to examine individual anomalies in detail. It can enhance the variations in the measured variables (Murphy, 2007). In areas of Uranium mineralization, Uranium is preferentially concentrated and, therefore, produces anomalously high Uranium/Thorium and Uranium/Potassium ratios (Wilkes, 1981). Radiometric ratios are often more reflective of lithological variation than the individual radiometric channels, hence a variety of radiometric ratio maps are produced. U/Th ratio has particular value in exploration for uranium deposits because it has been found to increase locally within regions containing uranium ores (Shiveset al., 1995). As thorium enrichment generally does not accompany potassium during hydrothermal alteration processes, the Th/K ratio provides an excellent distinction between potassium associated with alteration and anomalies related to normal lithological variations. It has been established that in general, low Th/K ratios are excellent indicators of Potassium alteration (Shiveset al., 1995).

$$X = \frac{U}{Th} \quad 1$$

$$Y = \frac{U}{K} \quad 2$$

$$Z = \frac{Th}{K} \quad 3$$

where X is the potassium, Y is the uranium and Z is the thorium used to represent the total count of the radioelements in the Oasis Montaj.

Ternary Radioelement Map

A ternary map is made by assigning one of the primary colours to each element's abundance. This map suggests to a great extent the lithological differences due to the color variations. The Uranium, Thorium, and Potassium maps emphasize regions where the specific radioelement has a total and pretty higher amount (Elawadiet al., 2004). Uranium, Potassium and Thorium are represented by blue, red and green respectively in generating the ternary map.

Gravity data analysis (regional and residual separation)

Polynomial fitting is the removal of the regional anomalies from the Bouguer gravity anomaly to obtain the residual anomalies. The residual component is due to relatively local near-surface masses while the regional component is that component of the total field arising from larger and deeper structures beneath the earth's surface. The extracted residual anomalies are often useful for structural mapping or qualitative interpretation based on visual inspection of the data. The resulting residual map might be a clear image of the anomaly so that qualitative interpretation may be carried out. Residual maps are also used extensively to bring into focus local features which tend to be obscured by the broad features of the regional field (Alagbe and Sunmonu, 2014).

Derivative

Derivatives help to sharpen the edges of anomalies and enhance shallow features (Revees, 2005). This includes first and second vertical derivatives and horizontal derivatives.

First vertical derivatives (FVD)

The first vertical derivative is an enhancement technique that sharpens up anomalies over bodies and tends to reduce anomaly complexity, thereby allowing clear imaging of the causative structures. The transformation can be noisy since it will amplify short-wavelength noise, that is, clearly delineates areas of different data resolution in the gravity grid (Revees, 2005).

$$FVD = -\frac{\partial A}{\partial Z} \quad 4$$

where A is the gravity field anomaly, equation 4 represent first vertical derivatives.

Second vertical derivatives (SVD)

The second vertical derivative emphasizes the expressions of local features and removes the effects of large regional influences or anomalies. As with other derivative displays, it is particularly helpful in the processing stage where it can be used to highlight line noise (Revees, 2005).

$$2VD = \frac{\partial^2 A}{\partial Z^2} \quad 5$$

where A is the gravity field anomaly, equation 5 represent second vertical derivatives

Horizontal Derivatives (HD)

This enhancement is also designed to look at fault and contact features. A maximum in the mapped enhancement indicates source edges. It is complementary to the filtered and first vertical derivative enhancements. It usually produces a more exact location for faults than the first vertical derivative. The HD method also has the characteristic of locating density contrast boundaries from gravity data (Grauch and Cordell, 1987; Fedi and Florio, 2001) and can delineate shallow and deep gravity sources. A maximum in the HDindicates the location offaults or contacts. The equation of the HD (Cordell and Grauch, 1985) is given as:

$$HD = \sqrt{(\frac{\partial A}{\partial x})^2 + (\frac{\partial A}{\partial y})^2} \quad 6$$

where A is the potential field anomaly

International Journal of Advances in Engineering and Management (IJAEM)
Volume 7, Issue 07 July 2025, pp: 331-348 www.ijaem.net ISSN: 2395-5252

Estimation of Depth to Basement (Sedimentary Thickness)

Source parameter imaging

The Source Parameter Imaging (SPI) is a quick, easy, and powerful method for calculating the depth of potential field sources. This technique developed by Thurston and Smith (1997) sometimes referred to as the local wavenumber method, is a profile or grid-based method for estimating potential field source depths. According to Thurston and Smith (1997), the SPI technique is represented mathematically by

$$\text{Depth} = \frac{1}{K_{max}} \quad (7)$$

where K_{max} is the maximum local wave number expressed in equation 8 as;

$$K_{max} = \sqrt{\left(\frac{\partial \text{Tilt}}{\partial x}\right)^2 + \left(\frac{\partial \text{Tilt}}{\partial y}\right)^2} \quad (8)$$

where the Tilt is given as

$$\text{Tilt} = \arctan \frac{\partial B/\partial z}{\sqrt{\left(\frac{\partial B}{\partial x}\right)^2 + \left(\frac{\partial B}{\partial y}\right)^2}} \quad (9)$$

where B = Bouguer, $\frac{\partial B}{\partial x}$, $\frac{\partial B}{\partial y}$, $\frac{\partial B}{\partial z}$ are the first-order partial derivates of the Bouguer in x, y and z coordinates.

Euler Deconvolution

The objective of the Euler deconvolution process is to produce a map that would show the nature and corresponding depths of the geologic sources observed in a two-dimensional grid (Whitehead and Musselman, 2005). The standard Euler 3-D method is based on the Euler homogeneity equation, an equation that relates the potential field and its gradient components to the location of the source, with the degree of homogeneity η which may be interpreted as a structural index SI (Thompson, 1982). The SI is an exponential factor corresponding to the rate at which the field falls off with distance, for a source of a given geometry. The standard 3-D form of Euler's equation (Reid, 1990) is expressed as:

$$x\frac{\partial B}{\partial x} + y\frac{\partial B}{\partial y} + z\frac{\partial B}{\partial z} + \eta B = x_0\frac{\partial B}{\partial x} + y_0\frac{\partial B}{\partial y} + z_0\frac{\partial B}{\partial z} + \eta b \quad (10)$$

where x, y and z are the coordinates of a measuring point, x_o, y_o and z_o are the coordinates of the source location whose total field is detected at x, y and z; b is a base level, η is structural index SI and B is potential field. The value of the SI depends on the type of source body one is investigating (Whitehead and Musselman, 2005). For example, η = 0, 1, 2 for a dyke or sill, cylinder and sphere (Thompson, 1982, Reid, 1990).

Forward and Inverse Modelling (Determination of Solid Minerals)

The potential field survey is used to detect bodies possessing unusual gravity properties, which reveal themselves by causing anomalies in the earth's gravitational field(Revees, 2005). Modelling techniques involve making numerical estimates of the depth and dimensions of the sources of anomalies and this often takes the form of modelling of sources which could, in theory, replicate the anomalies recorded in the survey. The forward and inverse modeling is a trial-and-error method. The shape, position and physical properties of the model are adjusted to obtain a good correlation between the calculated field and the observed field data. Using Potent Q software, the field of the model is calculated. Several profiles are taken on the residual gravity grid at different locations and modeled, each profile produces a degree of strike, dip and plunge where the observed values match well with the calculated values.

III. RESULTS AND DISCUSSION

Potassium Radiometric Map

Figure 1 is the potassium map revealing three different levels of K - concentrations that reflect different lithological units in the study area. The first level (low concentration) shown by blue to bright green colour ranging from lower values of 0.06 – 0.45 %, is dominant in the north-western (NW) parts of the study area (Agana and Oturpko) and is associated with carbonates(Oladunjoyeet al., 2014). The second level (intermediate concentration) represented by orange colours ranging from 0.45-0.60 % is associated with chemical sedimentary rocks and the third level (highest concentration) represented by pink colour ranging from 0.60-1.35 %, observed at the central portion (Gboko and Makurdi), southeastern, northeastern and northwestern directions is associated with mafic intrusive rocks(Oladunjoyeet al., 2014).

International Journal of Advances in Engineering and Management (IJAEM)
Volume 7, Issue 07 July 2025, pp: 331-348 www.ijaem.net ISSN: 2395-5252

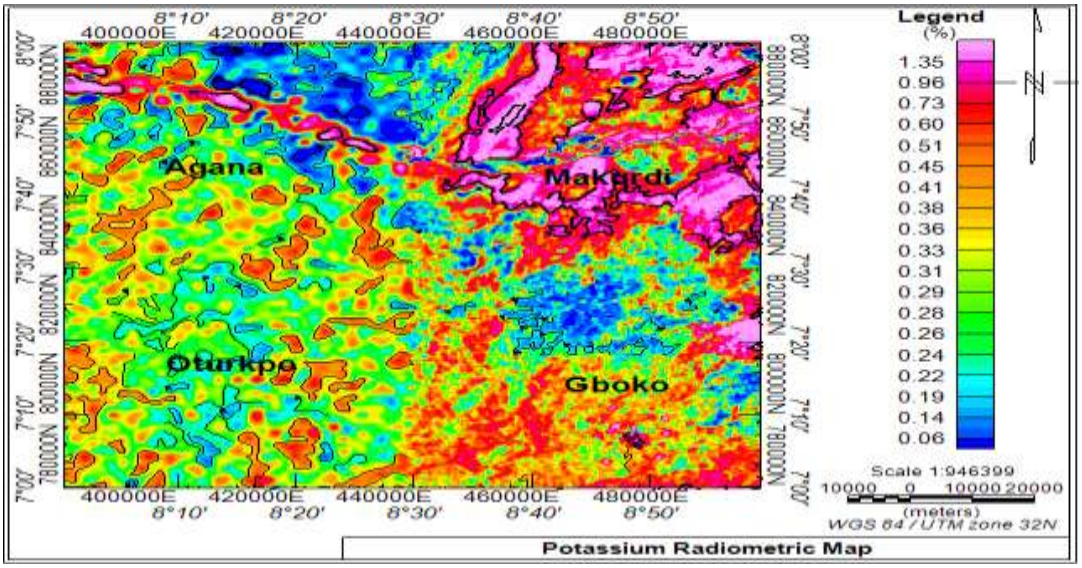

Figure 1: The Potassium Radiometric Map

Thorium Radiometric Map

The map of the Th concentration of the study area shown in Figure 2 displays three distinct regions of thorium concentrations. The map revealed a wide range of anomalies in the area. The study area is characterized by very high concentration region (first region) with values ranging from 15.5-18.9 ppm. The moderately high concentration region (second region) ranging from 11.1-15.5 ppm is associated with felsic intrusive rocks while low concentration region (third region) ranging from 1.8-11.1 ppm is associated with felsic extrusive rocks(Oladunjoyeet al., 2014). The high concentration regions are more observed at the northern boundaries, central portions and northwestern area (Agana and Oturkpo), while the low regions are noticed at the western portions (Makurdi and Gboko).

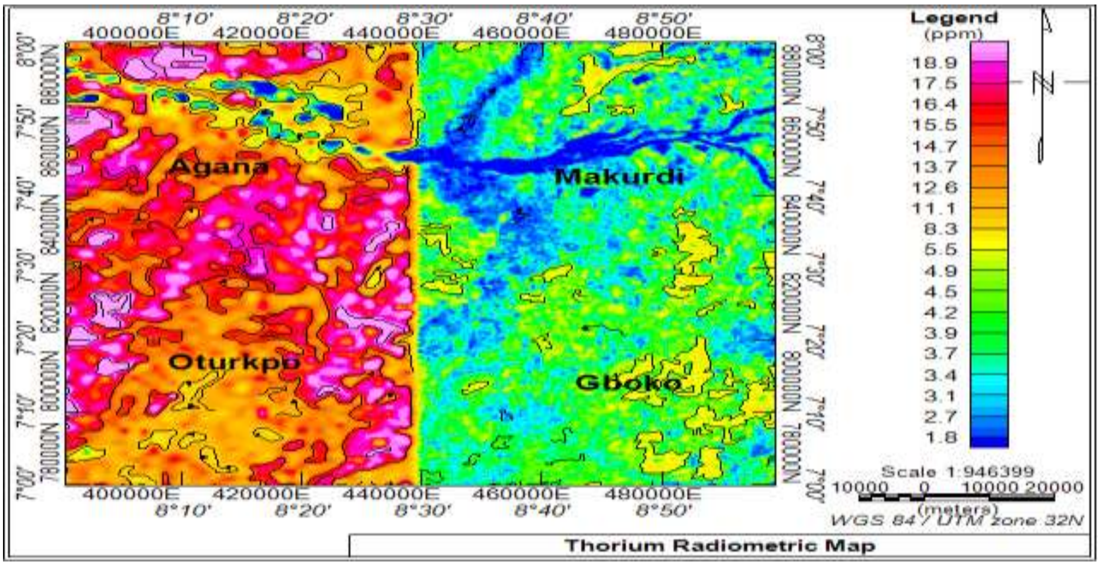

Figure2: The Thorium Radiometric Map

Uranium Radiometric Map.

Figure 3 is the map of U concentrations in the area showing three zones of concentration. The high concentration zones ranging from 16.2-19.8 ppm (pink colours) are associated with sedimentary rocks and the moderate concentration zones, with values ranging from 14.0-16.2 ppm are associated with felsic intrusive rocks. The low concentration

International Journal of Advances in Engineering and Management (IJAEM)
Volume 7, Issue 07 July 2025, pp: 331-348 www.ijaem.net ISSN: 2395-5252

zones (blue to bright green colours) ranging from 1.4 to 14.0 ppm is associated with metamorphic rocks(Oladunjoyeet al., 2014).

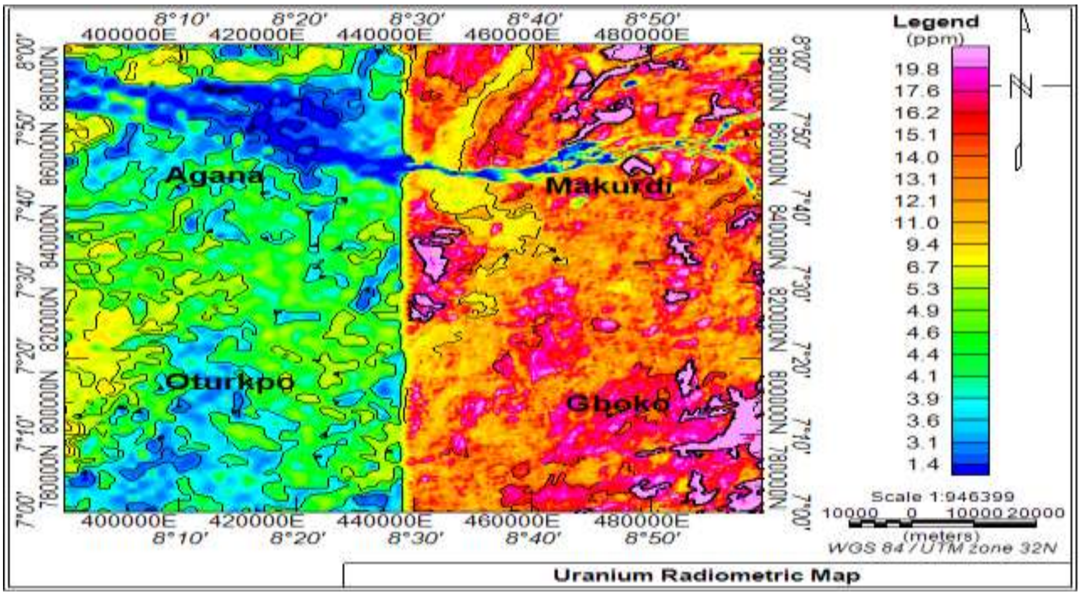

Figure 3: The Uranium Radiometric Map

Total Count of Radiometric Map

The total count map (Figure 4) revealed the combined effects of the radioactive elements (potassium, uranium and thorium) with the two major levels of radiation. The combined high concentrations (pink with orange colours) with values ranging from 1791.0-2422.8 cpt. The combined low concentrations (blue to green colours) with values ranging from 686.1-1791.0 cpt were observed at the western, northern and southeastern parts.

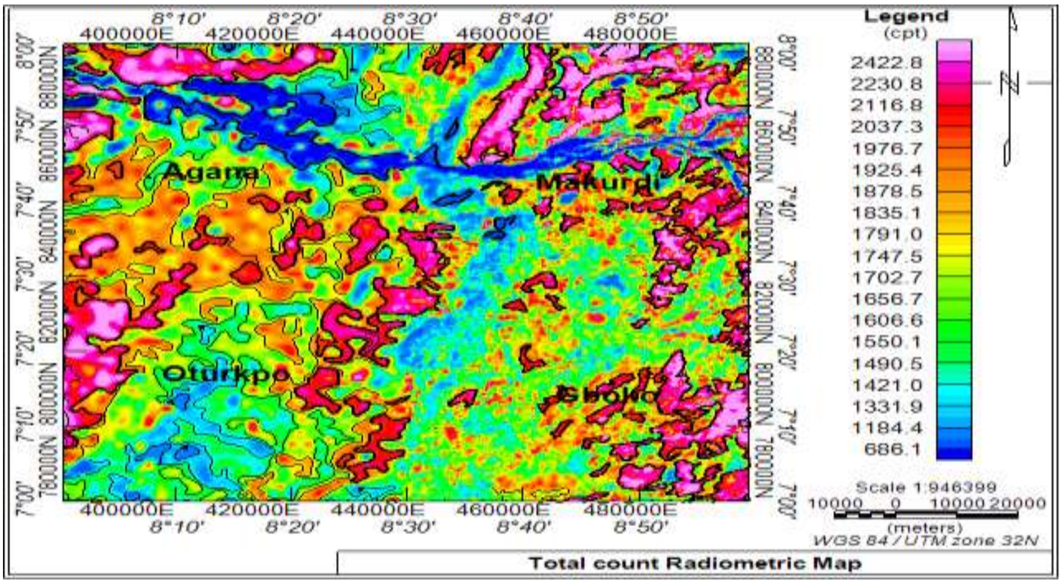

Figure 4: Total Count of Radiometric Map

Uranium/Potassium (U/K)Radiometric Ratio Map

The U/K radiometric ratio map was computed using Oasis Montaj (Figure 5). The high concentration of U/K radiometric ratio map which ranges from 40.7 to 92.1 ppm/% displayed a preferential enrichment of Uranium to Potassium mostly at the Gboko and Makurdiareas associated

International Journal of Advances in Engineering and Management (IJAEM)
Volume 7, Issue 07 July 2025, pp: 331-348 www.ijaem.net ISSN: 2395-5252

with weathered or leached associated with felsic and mafic rocks, (Wilfordet al. 1997). The intermediate concentration has values spanning from 24.0 – 40.7 ppm/%. The low concentration of U/K displayed latent concentration at Agana and Oturkpoareas with values ranging from 2.5-24.0 ppm/%.

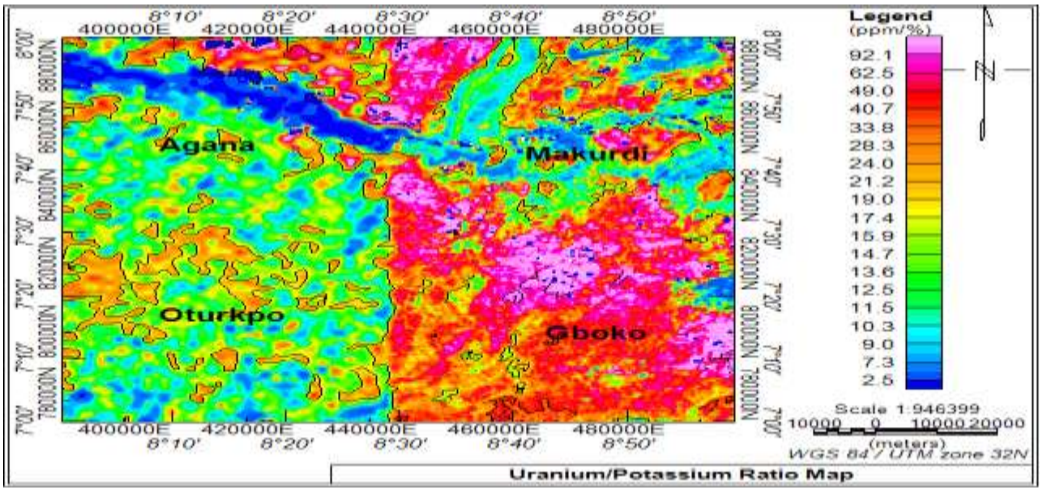

Figure 5: The U/K Radiometric Ratio Map

Uranium/Thorium (U/Th)Radiometric Ratio Map

The U/Th radiometric ratio map was computed using Oasis Montaj as shown in Figure 6. The high concentration of U/Th radiometric ratio map has values ranging from 4.10 to 4.91, while the intermediate concentration has values spanning from 3.50 to 4.10. The low concentration of U/Th has values ranging from 0.19 to 3.50. The colour legend bar shows high radiometric activities at Makurdi and Gboko (magenta) areas. The U/Th radiometric ratio map shows the preferential enrichment of thorium to uranium in the study area. Enrichment of uranium to thorium is observed at Makurdi and Gboko with their immobile nature.

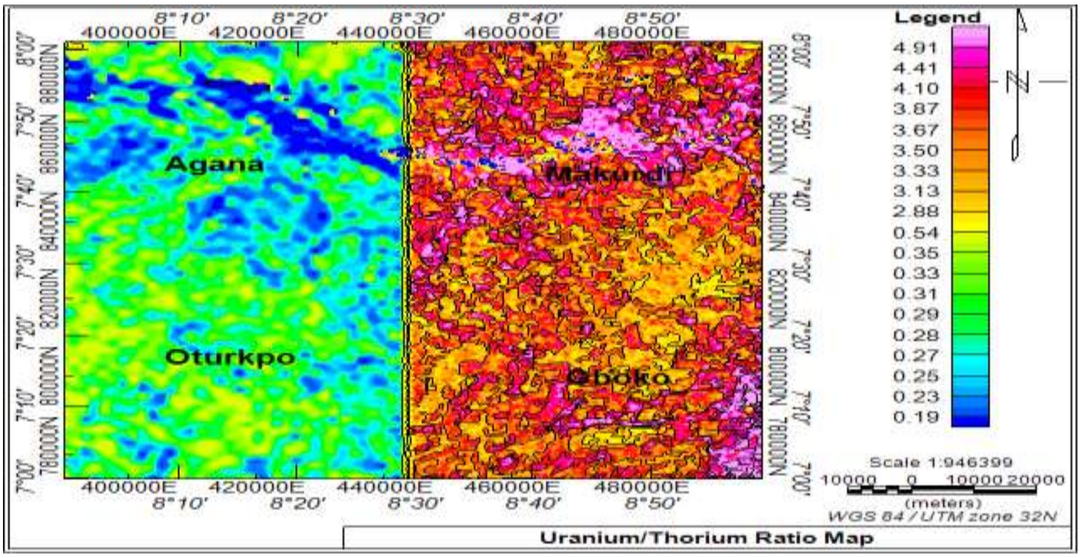

Figure 6: The U/Th Radiometric Ratio Map.

Thorium/Potassium (Th/K)Radiometric Ratio Map.

Figure 7 shows the Th/K radiometric ratio map. The high concentration of Th/K radiometric ratio map has values ranging from 58.9 to 82.8

International Journal of Advances in Engineering and Management (IJAEM)
Volume 7, Issue 07 July 2025, pp: 331-348 www.ijaem.net ISSN: 2395-5252

ppm/% at Agana and Oturkpo while the intermediate values range from 44.9 to 58.9 ppm/% with noticeable infiltration at Agana and Oturkpo. The low concentration of Th/K has values spanning from 1.6 to 44.9 ppm/%. The colour legend bar shows a high relative abundance of potassium to thorium at Agana and Oturkpo. High Th/K ratio signatures were observed at Agana and Oturkpo with hydrothermal alteration zones, which are characterized by encrichment in potassium(Adonuet al., 2022). Potassium is naturally more mobile than thorium.

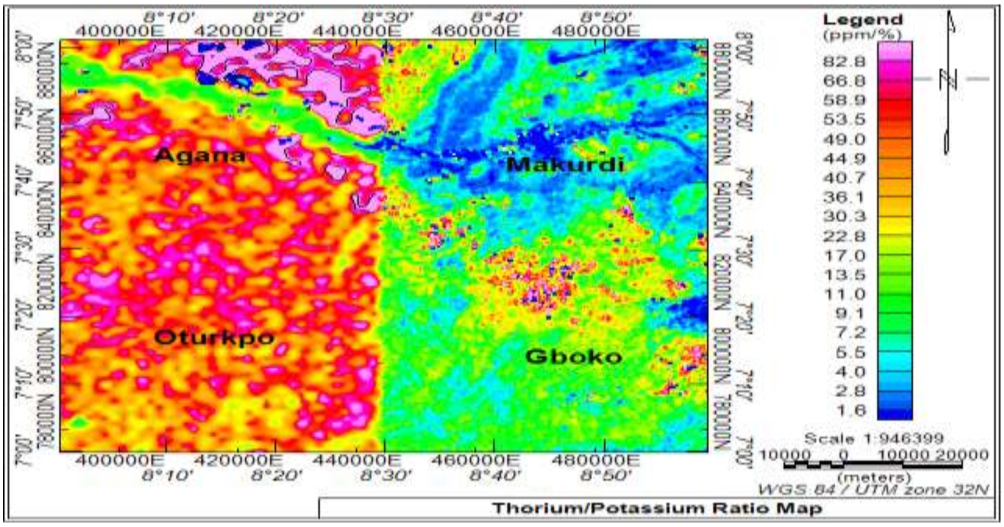

Figure 7: The Th/K Radiometric Ratio Map

Radiometric Ternary Map

The ternary map presented in Figure 8 illustrates the combined intensities of potassium (%K), uranium (ppm U) and thorium (ppm Th) in red, green and blue respectively. The black colour indicates low concentrations of (% K, ppm U and ppm Th) observed at Agana and parts of Oturkpo. The red colour corresponds to high potassium, low uranium and low thorium concentrations. The regions with a high concentration of thorium and a low concentration of uranium and potassium are displayed with green colours. The regions with high uranium, low potassium and thorium concentrations are characterized by blue colours while white colour areas are described as regions of high concentrations (Wilfordet al. 1997). Additionally, the areas showed with yellow colour indicate regions of high potassium, thorium and low uranium concentration, which depict possible alteration zones at Agana parts.

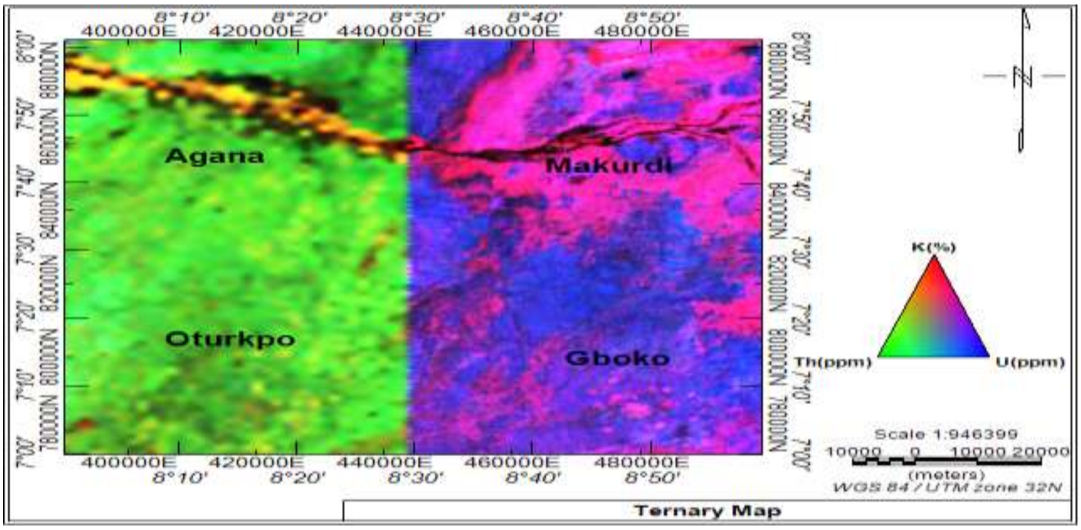

Figure 8: Radiometric Ternary Map

International Journal of Advances in Engineering and Management (IJAEM)
Volume 7, Issue 07 July 2025, pp: 331-348 www.ijaem.net ISSN: 2395-5252

Bouguer Gravity Map

The Bouguer anomaly of the study area varies from -37.8 to 10.7 mGal (Figure 9). The colour legend bar identifies Gboko regions of gravity high (red and pink) which corresponds to a region with high-density contrast beneath the surface. Intermediate values (green and yellow) and gravity lows (blue colour) correspond to regions of low-density contrast.

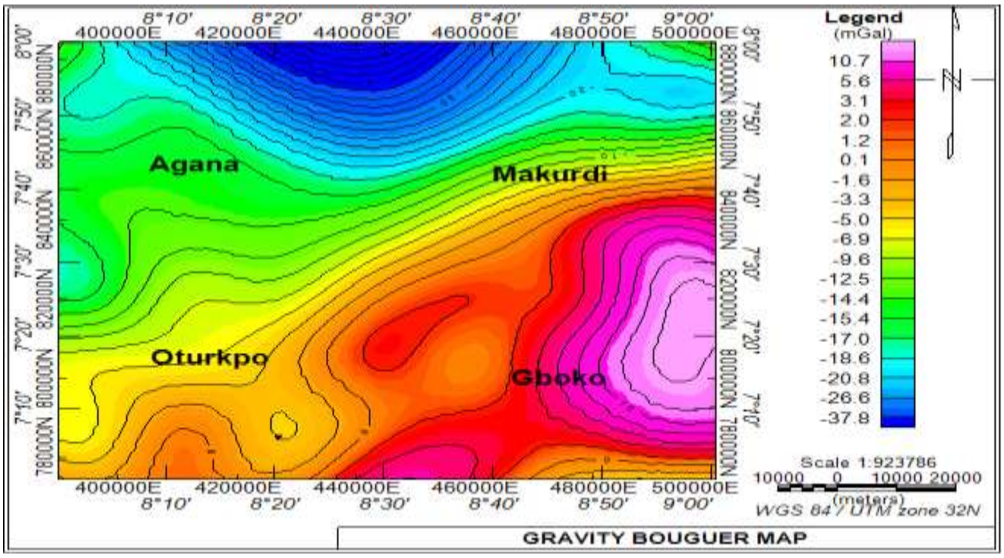

Figure 9: The Gravity Bouguer Map

Residual Bouguer Gravity

The residual Bouguer anomaly of the study area varies from -15.5 to 15.2 mGal (Figure 10). The colour legend bar identifies regions of gravity high (red and pink) which corresponds to regions with high-density contrast beneath the surface; intermediate values (green and yellow) and gravity lows (blue colour) that correspond to regions of low-density contrast.

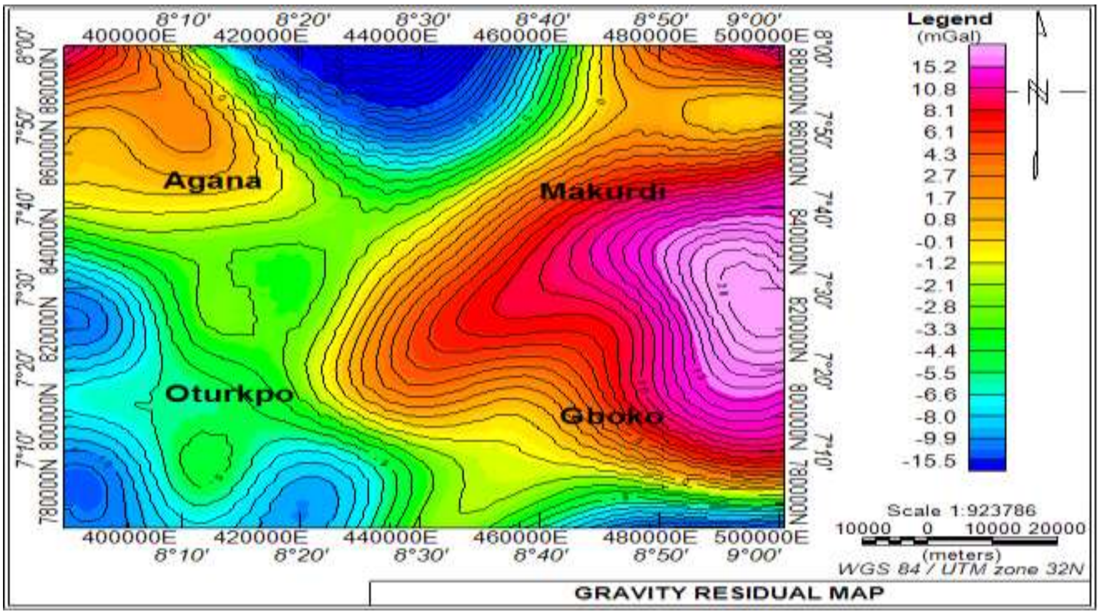

Figure 10: The Gravity Residual Map

International Journal of Advances in Engineering and Management (IJAEM)
Volume 7, Issue 07 July 2025, pp: 331-348 www.ijaem.net ISSN: 2395-5252

Regional Anomalies

The regional Bouguer anomaly of the study area varies from -24.0 to 6.8 mGal (Figure 11). The values decrease from the south to northern part of the study area indicating there is a fill of sediments more in the southern part than in the northern part.

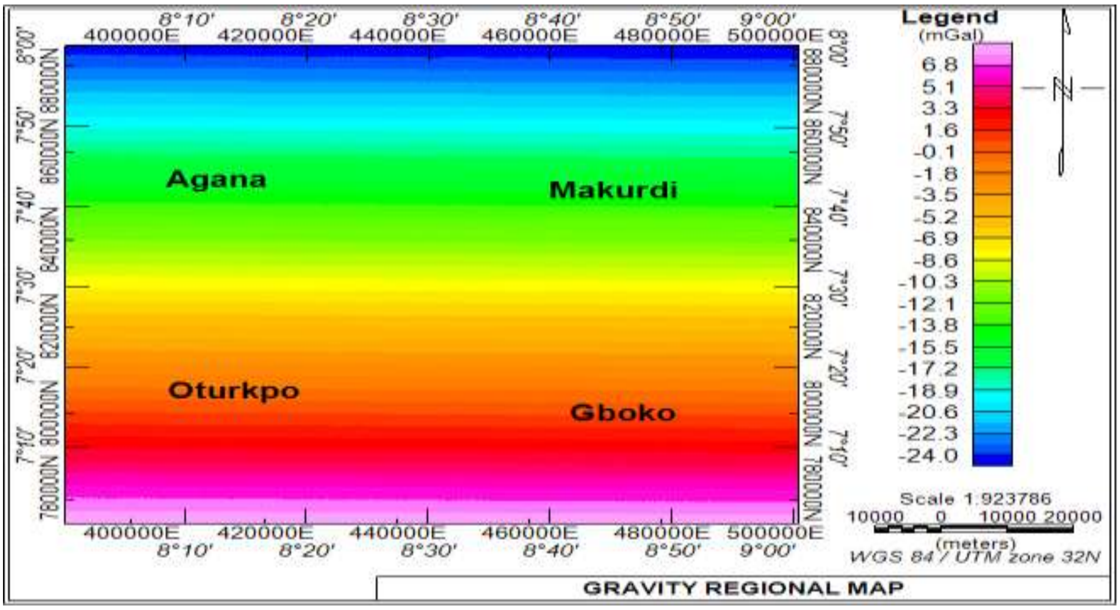

Figure 11: The Gravity Regional Map

First Vertical Derivative

Figure 12 is the first vertical derivative computed from Bouguer gravity data. The derivatives tend to sharpen the edges of the anomalies and enhance shallow features. The first vertical derivative of gravity map with values spanning from 0.00034 – 0.00057 mGal/m delineates regions with high-frequency features that indicate strong regional disturbance with large amplitude anomalies.The intermediate with values ranging from 0.00001 – 0.00034 mGal/m indicates regions with shallow features. The legend colour bar with values ranging from -0.00089 – 0.00001 shows regions with low-frequency anomalies.

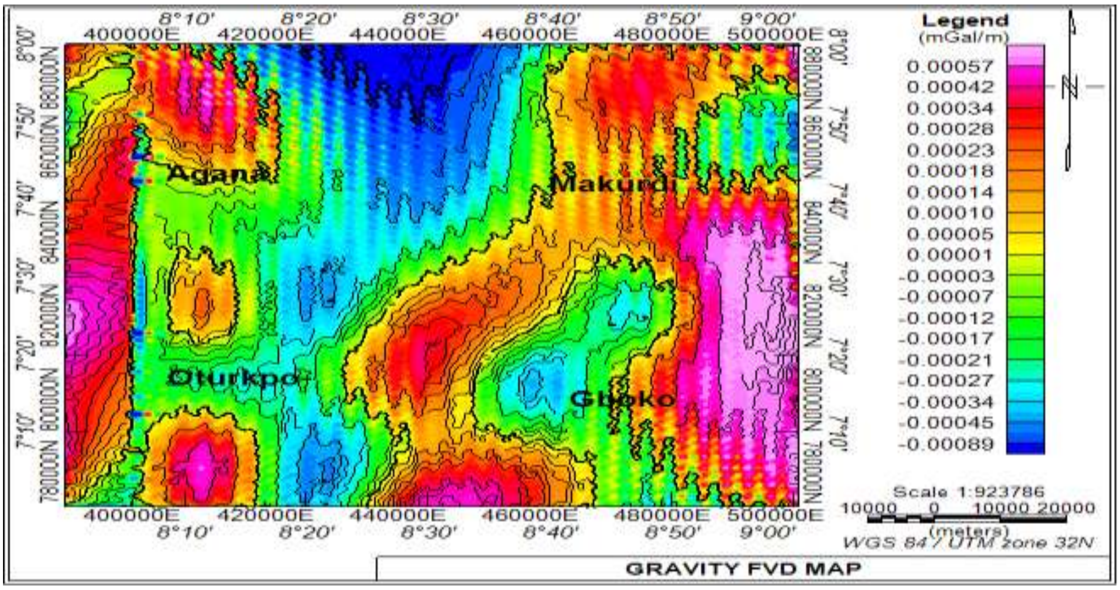

Figure 12: The First Vertical Derivative Map

Second Vertical Derivative

Figure 13 is the second vertical derivative of the gravity map. The legend bar colour with values ranging from -0.000000282 to 0.000000193 mGal/m expresses local features and the effects of large regional influences or anomalies. As with other derivative displays, it is particularly helpful in the processing stage where it can be used to highlight line noise.

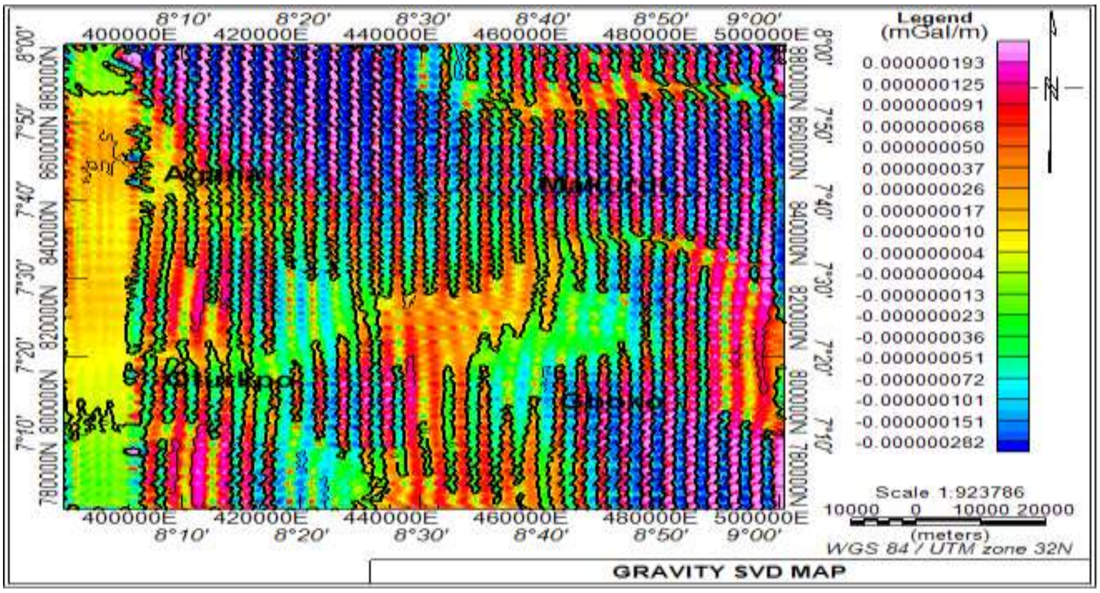

Figure 13: The Second Vertical Derivative Map

Horizontal Derivative

In Figure 14, the horizontal derivative was computed using Oasis Montaj software from Bouguer gravity data. The horizontal derivative is designed to look at fault and contact features. The legend bar with values ranging from 0.00046 to 0.00061 mGal/m indicates maxima in the mapped enhancement with source edges. It usually produces a more exact location for faults than the first vertical derivative with a characteristic of locating density contrast boundaries from gravity data and can delineate shallow and deep gravity sources(Igweet al., 2018).

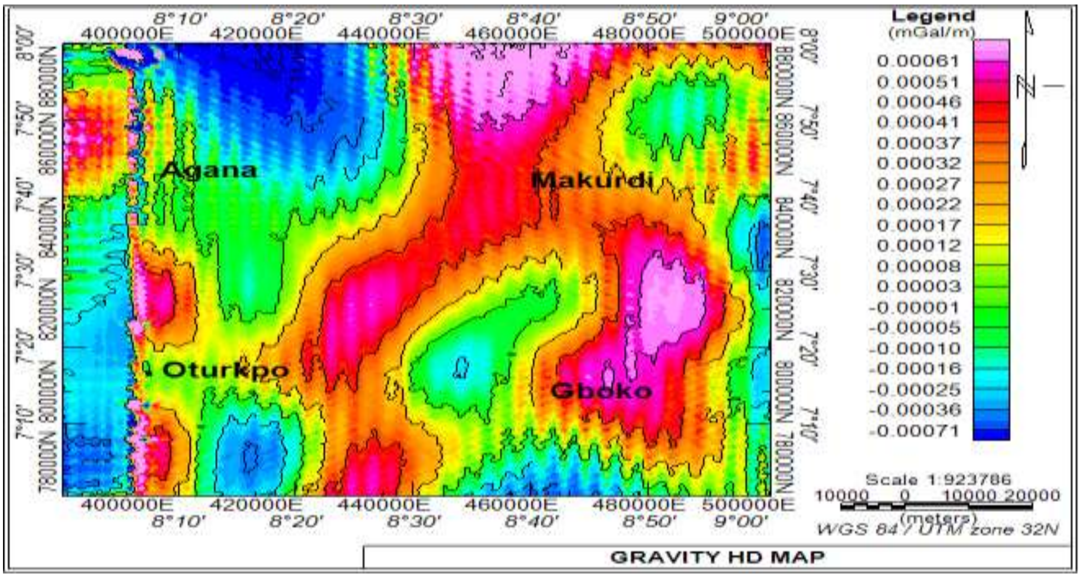

Figure 14: The Horizontal Derivative Map

International Journal of Advances in Engineering and Management (IJAEM)
Volume 7, Issue 07 July 2025, pp: 331-348 www.ijaem.net ISSN: 2395-5252

Source Parameter Imaging SPI

In computing the SPI depth of the gravity data, Oasis Montaj software was employed. Using the first vertical derivatives and horizontal derivatives, the SPI depth was computed. The negative depth values on the SPI legend depict the depths of buried bodies, which may be deep-seated basement rocks or near-surface intrusive. The pink colour generally indicates areas occupied by shallow gravity bodies, while the blue colour depicts areas of deep-lying gravity bodies. The SPI depth results for the gravity data range from -678.4 (shallow gravity anomalous bodies) to -4907.9 m (deep-lying gravity anomalous).

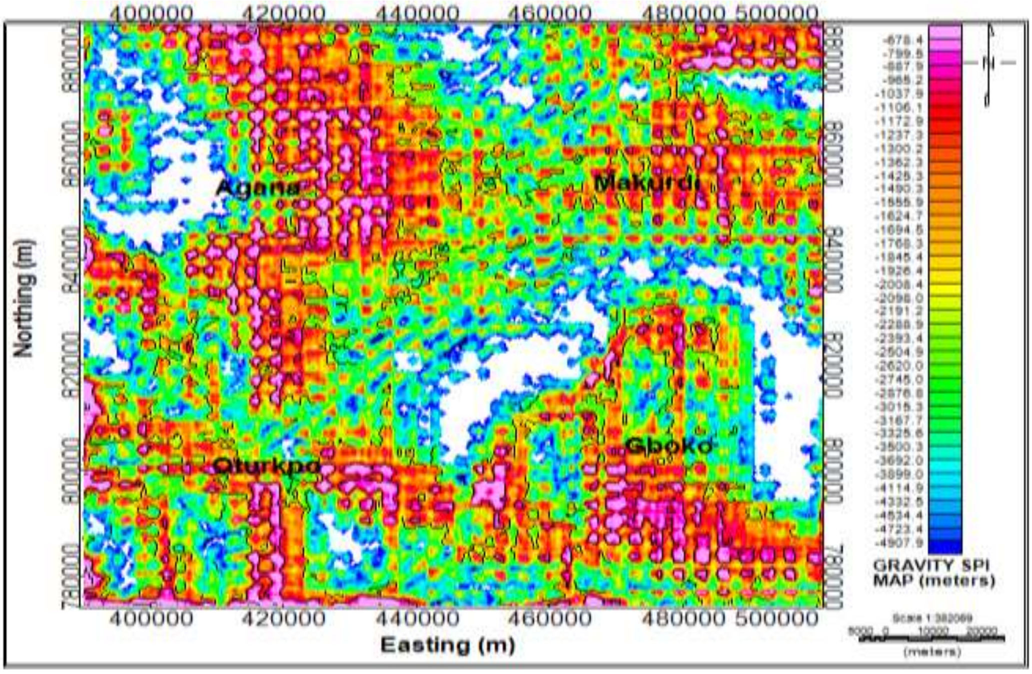

Figure 15: The Source Parameter Imaging

3D SPI Basement Topography

The computed deep depths of the basement were used to construct the 3D surface map for the basement topography of the area (Figure 16). The 3D surface map shows a linear depression with the thickest sediments in the northeastern region of the study area and an elevation with the shallowest sediments in the southwestern part of the study area.

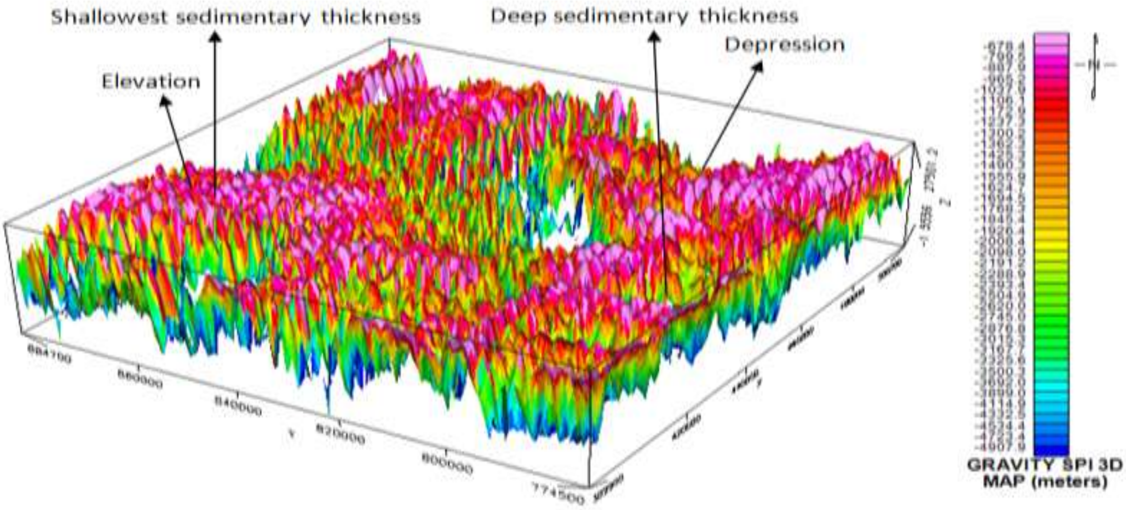

Figure 16: The 3D basement topography

International Journal of Advances in Engineering and Management (IJAEM)
Volume 7, Issue 07 July 2025, pp: 331-348 www.ijaem.net ISSN: 2395-5252

Euler Deconvolution

Oasis Montaj software was employed to compute the Euler depth for the different structural indices (SI= 0,1, 2). The Euler depths were estimated using vertical derivatives in three dimensions (x, y, and z). Vertical derivatives enhance shallow gravity bodies. Three Euler deconvolution maps were generated as shown in Figures 17(a-c) for the gravity data. The pink colour indicates shallow gravity bodies, while the blue colour indicates deep-lying gravity bodies. The results of Euler 3D depths are summarized in Table 1.

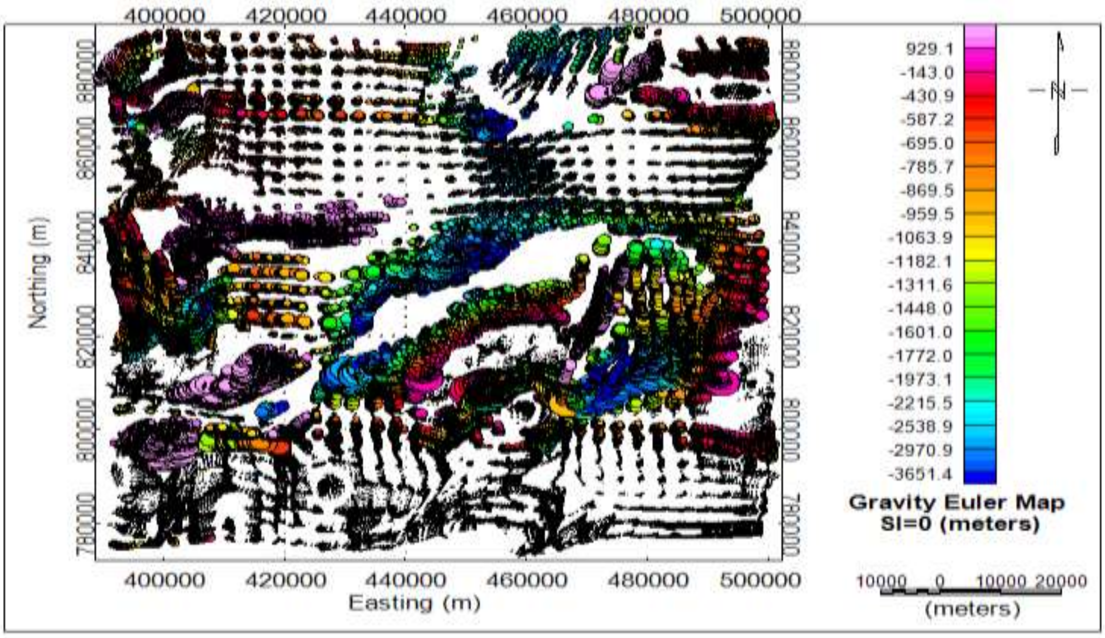

Figure 17a: The Gravity Euler Map SI = 0

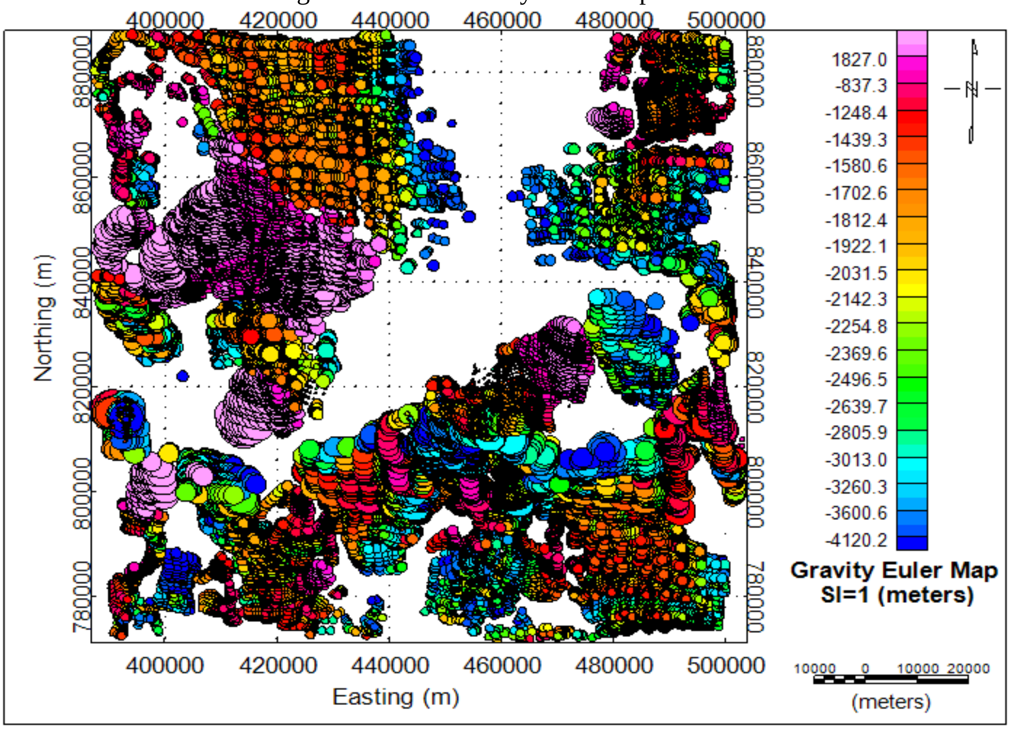

Figure 17b: The Gravity Euler Map SI = 1

International Journal of Advances in Engineering and Management (IJAEM)
Volume 7, Issue 07 July 2025, pp: 331-348 www.ijaem.net ISSN: 2395-5252

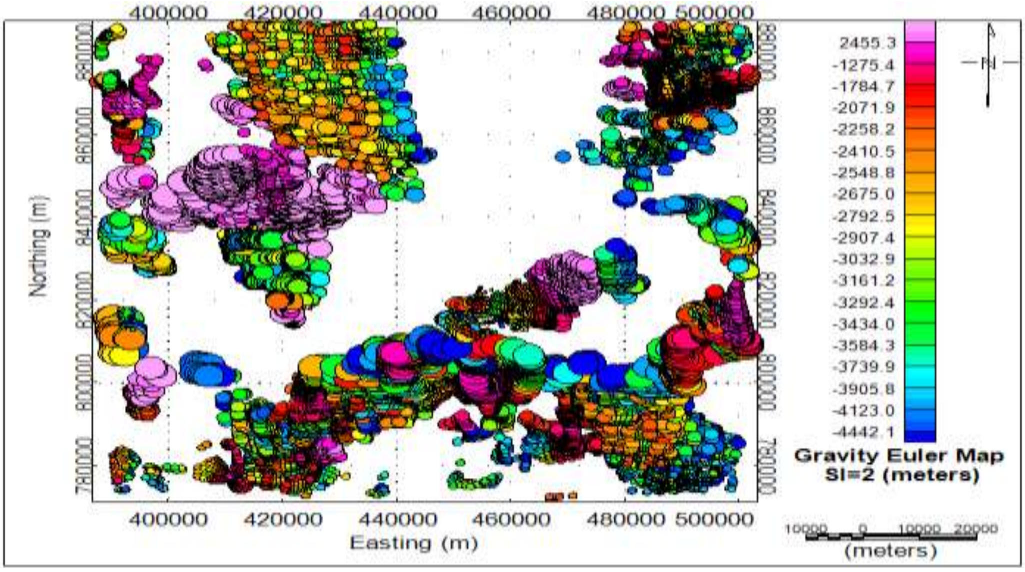

Figure 17c:The Gravity Euler MapSI = 2

Table 1: **Depth estimates for Euler-3D Deconvolution**

Structural Index, SI	Depth Ranges (m)
0	929.1 to -3651.5
1	1827.0 to -4120.2
2	2455.3 to -4442.1

Forward and Inverse Modeling

Four profiles were taken on the residual Bouguer grid (Figure 18) and modeled. The profile produced a degree of strike, dip, and plunge where the observed values matched well with the calculated values (Figures 4.19a-d). The blue curves represent the observed field values while the red curves represent the calculated field values. The forward modeling being a trial-and-error method; the shape, position and physical properties of the model were adjusted in order to obtain a good correlation between the calculated field and the observed field. The results of the forward and inverse modeling are summarized in Table 2.

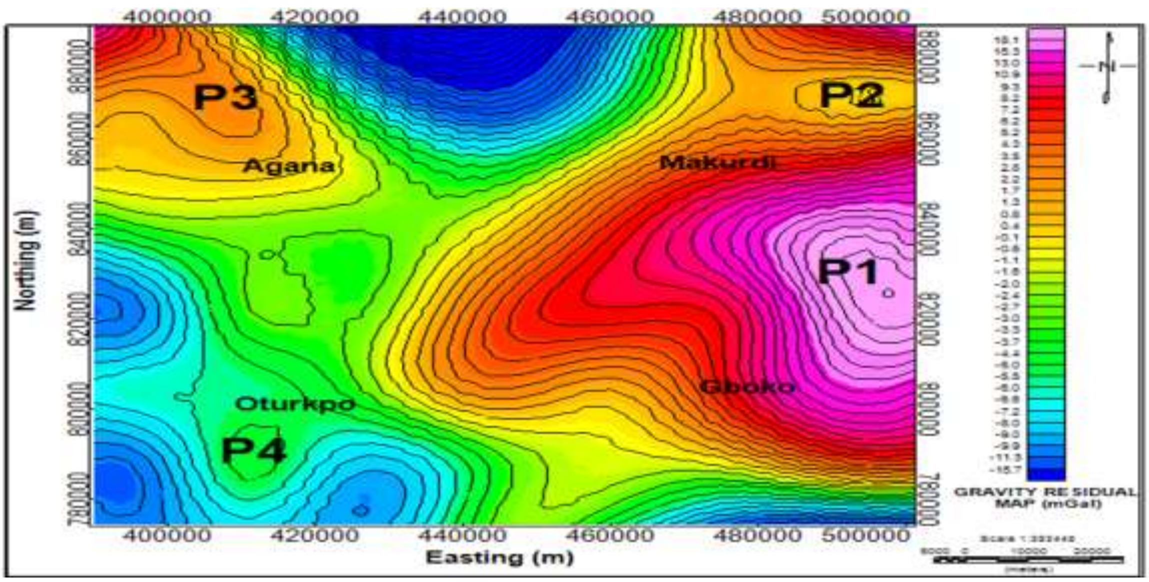

Figure 18: The Gravity Residual Contour Map

International Journal of Advances in Engineering and Management (IJAEM)
Volume 7, Issue 07 July 2025, pp: 331-348 www.ijaem.net ISSN: 2395-5252

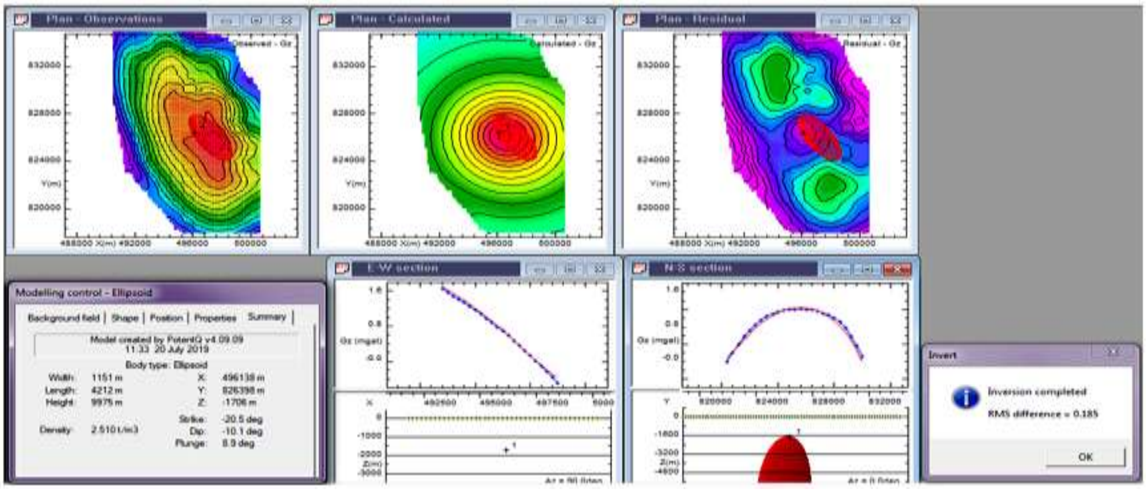

Figure 19a:The Profile 1 Modeled

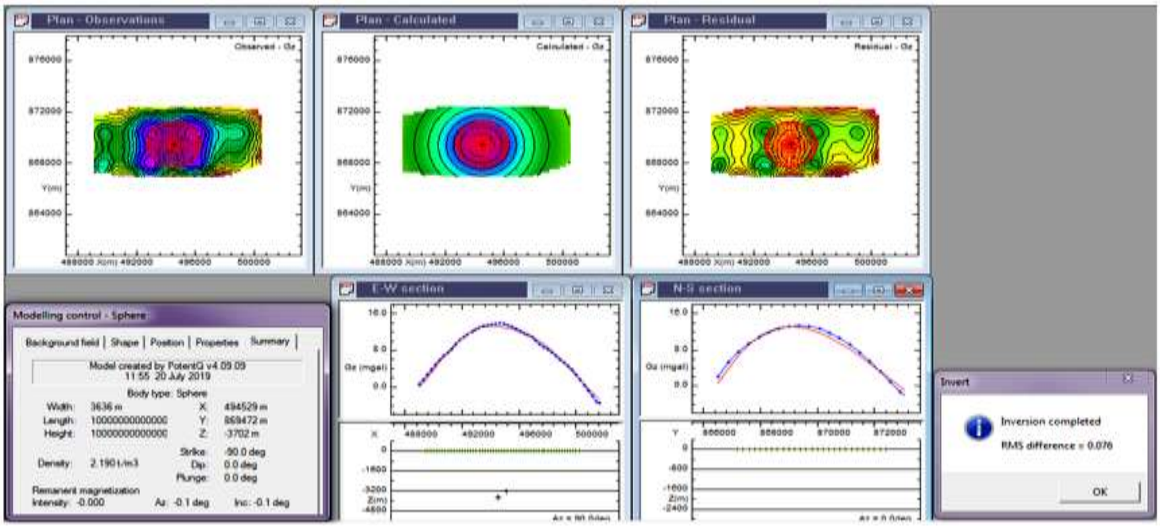

Figure 19b:The Profile 2 Modeled

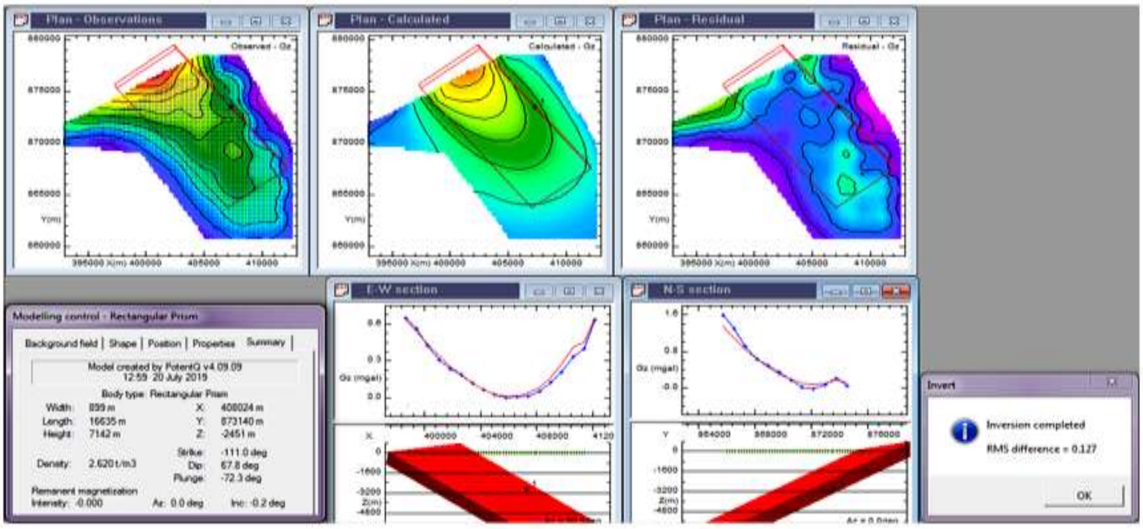

Figure 19c:The Profile 3 Modeled

International Journal of Advances in Engineering and Management (IJAEM)
Volume 7, Issue 07 July 2025, pp: 331-348 www.ijaem.net ISSN: 2395-5252

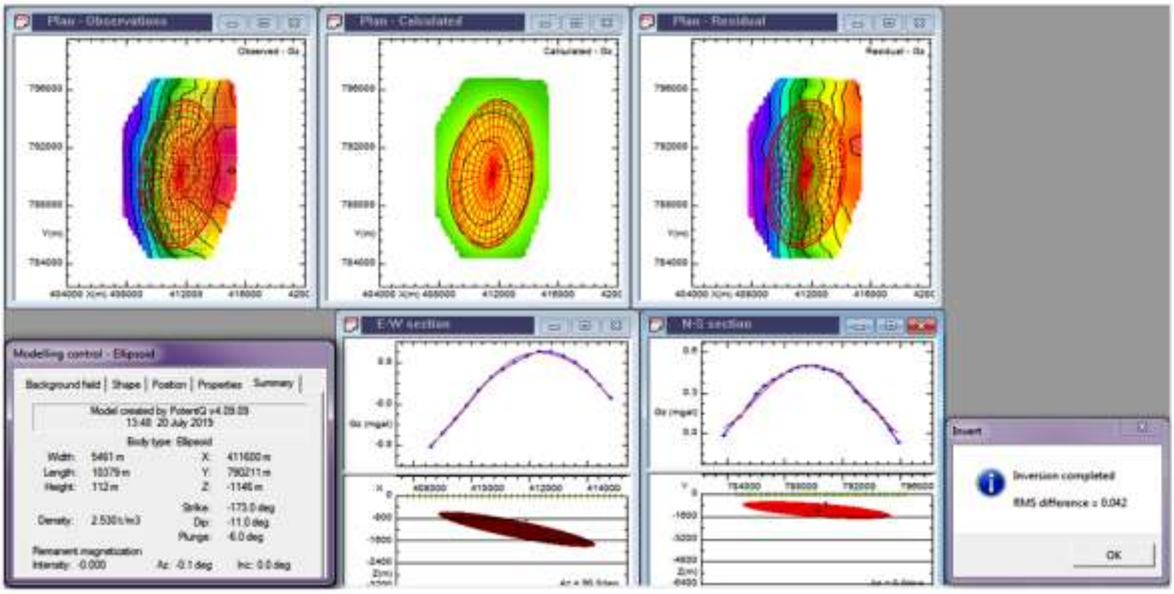

Figure 19d:The Profile 4 Modeled

Table 2 **Summary of Gravity Forward and Inverse Modeling Results.**

Model	Model shape	X(m)	Y(m)	Depth to anomalous body (m)	Plunge (deg)	Dip (deg)	Strike (deg)	Density value (g/cm^3)	Possible cause of the anomaly
P1	Ellipsoid	496138	826398	-1706	8.9	-10.1	-20.5	2.51	Shale, Clay (Gboko)
P2	Sphere	494529	869472	-3702	0.0	0.0	-90.0	2.19	Shale, Limestone (Makurdi)
P3	Rectangular Prism	408024	873140	-2451	-72.3	67.8	-111.0	2.62	Limestone, Shale, Sandstone (Agana)
P4	Ellipsoid	411600	790211	-1146	-6.0	-11.0	-173.0	2.53	Sandstone, Shale (Oturkpo)

IV. CONCLUSION

The integrated airborne radiometric and gravity data of the study area have been interpreted qualitatively and quantitatively. The radiometric maps of potassium, uranium, and thorium, ratio maps, total count radiometric, and ternary analysis were employed in the qualitative and quantitative interpretation to determine zones of concentration of the radiometric anomalies and radioelement mineralization in the area. The maximum gravity SPI and Euler depths are -4907.9 m and -4442.1 m respectively. The depths from SPI and Euler deconvolution are in close agreement. The radiometric ratio analysis and the 3D gravity modelling revealed the presence of rock bearing minerals in the study area which are; granite, limestone, shale, clay, and sandstone. Therefore, the research area has identified rock bearing mineral deposits that could be utilized as raw material(s) by numerous companies and industries in Nigeria. The maximum sedimentary thickness of 4907.9 m obtained indicates the possibility of hydrocarbon accumulation and exploration in the area.

ACKNOWLEDGEMENTS

The authors appreciate the work of the editors and reviewers. They appreciate in a special way the Nigerian Geological Survey Agency and National Aeronautics and Space Administration for providing data for this work.

REFERENCES

[1]. Adonu, I.I, Ugwu, G.Z. and Onyishi, G.E. (2022).Interpretation of Airborne Radiometric Data of Part of Middle Benue Trough of Nigeria for Mineral Deposits.IOSR Journal of Applied and Geology and Geophysics, 10(1): 59 – 62.

[2]. Alagbe, O. A. and Sunmonu, L. A. (2014). Interpretation of Gravity Data from Upper Benue Basin, Nigeria Using Automated Techniques. IOSR Journal of Applied Geology and Geophysics, 2: 22 - 40.

[3]. Cordell, L. and Grauch, V.J.S. (1985) Mapping Basement Magnetization Zones from Aeromagnetic Data in the San Juan Basin, New Mexico. In: Hinze, W.J., Ed., The Utility of Regional Gravity and Magnetic Anomaly Maps, Society of Exploration Geophysicists, 181-197. http://dx.doi.org/10.1190/1.0931830346.ch16.

[4]. Elawadi, E., Ammar A. and Elsirafy, A. (2004). Mapping surface geology using airborne gamma ray spectrometric survey data - A case study. Proceedings of SEGJ international symposium. Nuclear Materials Authority of Egypt, Airborne Exploration Dept.

[5]. Fatoye, F.B and Gideon, Y. B (2013). Geology and mineral resources of the Lower Benue Trough Nigeria (Pelagia Research Library). Coden (USA), 4(6): 21 – 28.

[6]. Fedi, M. and Florio, G. (2001) Detection of Potential Fields Source Boundaries by Enhanced Horizontal Derivative Method. Geophysical Prospecting, 49, 40-58. http://dx.doi.org/10.1046/j.1365-2478.2001.00235.x

[7]. Grauch, V.J.S. and Cordell, L. (1987) Limitations of Determining Density or Magnetic Boundaries from the Horizontal Gradient of Gravity or Pseudogravity Data. Journal of Geophysics, 52, 118-121. http://dx.doi.org/10.1190/1.1442236

[8]. Igwe, E.A, Yakubu, J.A. and Idike, J.I. (2018).Investigation of Nsukka area South Eastern Nigeria for Mineral exploration using gravity method.IOSR Journal of Applied Physics (IOSR-JAP),10(2): 22 - 32.

[9]. Lowrie, W. (2007).Fundamentals of Geophysics. Cambridge University Press, London.

[10]. Murphy, B.C.R. (2007). Airborne Geophysics and the Indian scenario. Journal of Industrial Geophysics, 11(1): 1-28.

[11]. Oladunjoye, M.A, Akinmosin, A. and Ekugum, U.K. (2014). Distribution of radioactive elements of some rocks in Southwestern Nigeria, 61: 231 – 240

[12]. Revees, C. (2005). Aeromagnetic Surveys; Principles, Practice and Interpretation.GEOSOFT, 155.

[13]. Reid, A. B. (1980). Aeromagnetic survey design. Geophysics, 45: 973-976.

[14]. Shives, R. B. K., Ford, K. L., and Charbonneau, B. W. (1995). Applications of gamma-ray spectrometric/magnetic/VLF-EM surveys— Workshop manual: Geol. Surv. Can. Open File 3061.

[15]. Telford, W. M., Geldart, L. P. and Sheeriff, R. E. (1990). Applied geophysics ($2nd$ edition). Cambridge University press, Cambridge.

[16]. Thompson, D. T. (1982). A new technique for making computer-assisted depth estimates from Magnetic data. Geophysics, 47(1): 31-37.

[17]. Thurston, J. B. and Smith, R. S. (1997). Automatic conversion of magnetic data to depth, dip,and susceptibility contrast using the SPITM method. Geophysics, 62(3): 807-813.

[18]. Whitehead, N. and Musselman, C. (2005). MontajTMGrav/Mag interpretation: Processing,Analysis and visualization system for 3D inversion of potential field data for OasismontajVol 6.1. Geosoft Inc. ON, Canada.

[19]. Wilkes, P. G. (1981). Acquisition, Processing, and Interpretation of Airborne Gamma-ray Spectrometry Data. Bureau of Mineral Resources and Mining, Geology and Geophysics, Report, 186: 48 – 49.

[20]. Wilford, J. R., Bierwirth, P. N. and Craig, M. A. (1997). Application of airborne gamma-ray spectrometry in soil/regolith mapping and applied geomorphology. AGSO Journal of Australian Geology and Geophysics; 17(2):201-216.